PERGAMON

International Journal of Multiphase Flow 25 (1999) 1305–1319

International Journal of Multiphase Flow

www.elsevier.com/locate/ijmulflow

Flow characteristics and circulatory motion in wavy falling films with and without counter-current gas flow

G. Karimi, M. Kawaji*

Department of Chemical Engineering and Applied Chemistry, University of Toronto, Toronto, Ont. Canada M5S 3E5

Received 8 December 1998; received in revised form 13 April 1999

We would like to congratulate Professor Gad Hetsroni on his 65th birthday and wish him good health and happiness for many years to come. As both authors and readers of the Journal articles, we sincerely appreciate Gad's immense contributions, as editor of the Journal, to the dissemination of the latest results in multiphase flow research throughout the international scientific community.

Abstract

A laser-induced photochromic tracer technique was used to investigate the flow structure in a thin, wavy falling liquid film in a vertical tube both with and without interfacial shear induced by a counter-current flow of gas. Instantaneous velocity profile and film thickness were measured simultaneously to better understand the turbulence characteristics and the enhancement effect of interfacial waves and shear on the heat and mass transfer rates. While surface ripples were found to exert almost no influence on the near-wall hydrodynamics, the large wave effects could easily be sensed close to the solid wall, altering the turbulence intensity profiles. Flow visualization experiments revealed the occurrence of circulatory motions with significant velocities normal to the tube wall under the large waves, which may be the dominant mechanism for wall-to-liquid and interfacial transport phenomena for wavy films. © 1999 Elsevier Science Ltd. All rights reserved.

Keywords: Flow characteristics; Circulatory motion; Wavy falling films; Counter-current gas flow

* Corresponding author. Tel.: +1-416-978-3063; fax: +1-416-978-8605.
E-mail address: kawaji@ecf.utoronto.ca (M. Kawaji)

PII: S0301-9322(99)00044-0

1. Introduction

The transport characteristics of liquid films are of great practical importance in many industrial applications. At flow rates of industrial interest, falling liquid films are likely turbulent and characterized by the presence of waves at the film surface. Understanding of the effects of these waves is very important in predicting the heat and mass transfer rates in falling film devices because it is well known that the surface waves can drastically enhance transfer of momentum, heat and mass across the gas–liquid interface and at the wall-liquid boundaries.

Compared to heat transfer, mass transfer in liquid films is a slower process due to different physical mechanisms involved. This suggests that mass transfer rates are more sensitive to wave-induced fluctuations in the flow field than heat transfer rates. Therefore, it is important to clarify the mass transfer mechanism in relation to interfacial wave characteristics and turbulence structure on the liquid side.

Considerable efforts have been devoted to the prediction of gas absorption into falling liquid films and numerous theoretical and empirical models have been published in the literature. However, the problem is difficult due to the stochastic nature of the interfacial waves and the complexity of the turbulent mixing motion in the liquid near the gas–liquid interface. Hence, no uniformly accepted method for the prediction of mass transfer rates has yet been proposed.

Experimentally, Emmert and Pigford (1954), Kamei and Oishi (1955), Lamurelle and Sandall (1972), Chung and Mills (1976), Henstock and Hanratty (1979), Yih and Chen (1982), among others, measured rates of gas absorption in free falling films. Indeed, Emmert and Pigford (1954) were the first to show manyfold enhancement of mass transfer due to the waves during absorption and desorption of O_2 and CO_2 in a falling water film, in the range of $Re_L = 100–1800$. Seban and Faghri (1978) reviewed experimental data on the absorption rates and found that the absorption rates for wavy films are up to several times larger than the rates calculated for smooth films, even for laminar flow.

The mechanism by which the waves increase the mass transfer rate to such an extent, much larger than the approximately 20–30% increase in heat transfer rate, is not fully clear. In addition, the interfacial area increases only slightly due to the waves that obviously cannot be responsible for such mass transfer augmentation. Therefore, other mechanisms such as local mixing and surface renewal motion under the waves may be the most important contributor to the enhanced transfer rates. Karimi and Kawaji (1998) have recently reported on the internal hydrodynamics of freely, wavy turbulent films determined using a flow visualization method called photochromic dye activation technique. Wave-induced turbulence was found to produce flat velocity profiles in large amplitude waves, and to affect the flow structure in thin substrate film depending on the wave amplitude.

On the other hand, there have also been many attempts to model the mass transfer processes across gas–liquid interfaces. A variety of models of various complexities have been proposed, particularly in open channel flow systems. Higbie's (1935) penetration model, Fortescue and Pearson's (Fortescue and Pearson, 1967) eddy cell model and recently, a hybrid eddy cell-surface renewal model proposed by Komori et al. (1993) are a few examples. A fewer number of studies have been reported for falling liquid films (e.g., Banerjee et al., 1967; Wasden and Dukler, 1992; Yoshimura et al., 1996). However, even the most sophisticated of these models relies on some kind of hypotheses for transport mechanisms and requires empirical inputs in the form of constants or functions. Indeed, these models may not simulate the real physical phenomena, which occur within the wavy falling liquid film. Therefore, the lack of understanding of the hydrodynamics and the transport mechanisms has made these models limited in accuracy and range of applicability.

In this paper, several new findings on the flow structure of wavy liquid films are presented focusing on the dominant hydrodynamics, to better understand their relevance to the enhanced heat and mass transfer rates in wavy falling liquid films. The present study attempts to assess the role of interfacial waves in mass transfer in falling liquid films through an examination of instantaneous velocity profiles and turbulence characteristics under the wavy film both with and without a counter-current gas flow.

2. Experimental apparatus and measurement techniques

The experimental apparatus used is shown in Fig. 1. It was the same as that described by Karimi and Kawaji (1996, 1998), and only the main features are presented here. The test section consisted of a 2.44 m long, Pyrex vertical tube with an ID of 50.8 mm. The liquid flow loop contained deodorized kerosene, with a photochromic dye (TNSB) dissolved at a

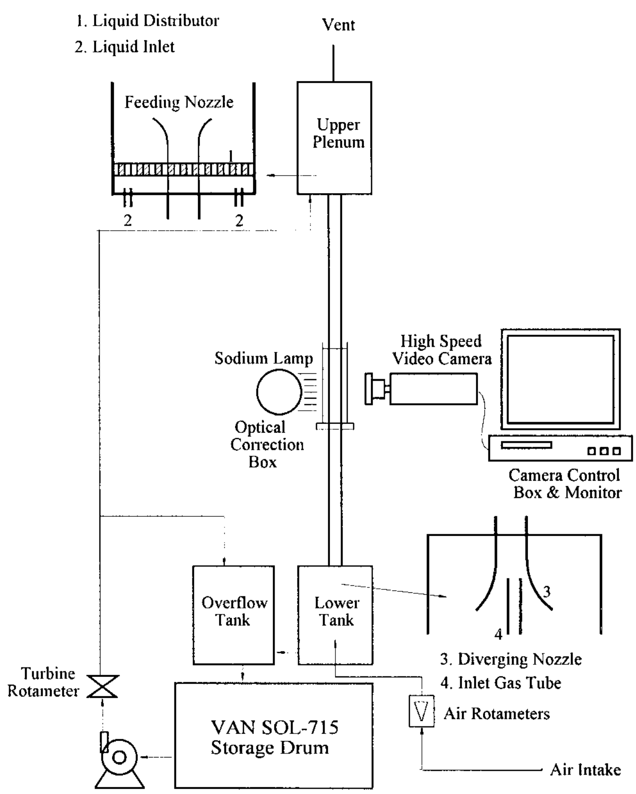

Fig. 1. Flow loop diagram.

concentration of 0.01% by weight to conduct simultaneous measurements of velocity profile and film thickness. Kerosene entered the test section by smoothly overflowing into a converging nozzle and forming a falling liquid film of uniform thickness. The liquid was discharged from the bottom of the test section through a diverging nozzle. Air at a controlled flow rate was injected from the bottom of the test section through an 8 mm ID stainless steel tube aligned with the tube axis.

The liquid flow was investigated over a wide range of liquid and gas Reynolds numbers at two different locations, 50 and 150 cm from the liquid entrance. To investigate the effect of counter-current interfacial stress, the airflow rate was set to a value just below the onset of flooding. The liquid and gas Reynolds numbers, Re_k, are calculated here as $Re_k = \rho_k j_k D/\mu_k$, where j_k is superficial velocity ($4Q_k/\pi D^2$), ρ_k is density and μ_k is the dynamic viscosity of phase k, and D is tube inside diameter. The subscript, k, stands for liquid, L, or gas, G.

The instantaneous velocity profiles in the wavy falling liquid films have been measured using a photochromic dye tracer technique. This visualization technique is based on an instantaneous reaction of a photochromic dye material dissolved in the liquid with a high intensity ultraviolet laser beam. The motions of traces formed were recorded using a high speed CCD camera at a rate of 744 frames per second. Background lighting was provided by a 1 kW sodium lamp whose light intensity was adjusted to provide sharp contrast between the photochromic dye traces and the test fluid.

Digital images recorded by the CCD camera were then reviewed frame by frame, and the trace containing images were captured using a video frame grabber card installed on a personal computer. The digitized data, which indicate the trace positions in different frames, were used to determine the velocity profiles by dividing the trace displacement by the elapsed time interval.

The experiments were conducted under conditions summarized in Table 1. A variety of flow conditions were studied; a smooth-laminar falling liquid film in a developing flow region ($L = 50$ cm), wavy-laminar, laminar-to-turbulent transition and wavy-turbulent liquid films in a developed flow region, $L = 150$ cm. The effect of counter-current interfacial shear on liquid film flow was also investigated, by imposing an upward flow of air at near atmospheric pressure and flow rates just below the values needed to cause flooding.

Table 1
Summary of experimental conditions

Run	Measuring location (cm)	Re_L	Re_G	$\bar{\delta}$ (mm)	RMS	Regime
1	50	2352	–	1.07	0.064	Smooth-laminar
2	50	2652	11,703	1.09	0.237	Onset of flooding
3	150	1408	–	0.56	0.131	Wavy-laminar
4	150	3331	–	1.06	0.147	Transition
5	150	3331	10,701	0.97	0.267	Onset of flooding
6	150	5275	–	1.37	0.419	Wavy-turbulent

3. Experimental results

Hydrodynamic structures along with the interfacial wave characteristics of falling liquid films over a wide range of liquid and gas flow conditions have been given in detail in Karimi and Kawaji (1996, 1997, 1998). In this paper, liquid film's hydrodynamic structures and turbulence characteristics relevant to the heat and mass transfer augmentation in such systems will be presented and discussed.

3.1. Interfacial waviness and stream-wise velocity fluctuations

In this work, simultaneous and local stream-wise velocity variations and film thickness fluctuations are presented. This type of information would help answer fundamental questions such as how far wave-induced momentum could penetrate into the liquid film. Obviously, transfer of momentum is related to the transfer of mass and heat.

Fig. 2a–d illustrate simultaneous time profiles of film thickness fluctuations and local stream-wise velocities at different normalized distances from the wall, $y/\bar{\delta}$, in freely falling films (no gas flow) under different flow conditions (Runs 1, 3, 4 and 6). The time-averaged film thickness is shown by a dashed line in each run. The stream-wise velocities at various distances from the wall were obtained from the measured instantaneous velocity profiles. The gaps in the velocity data especially near the wavy interface, resulted from passage of wave troughs and sudden contraction of the film thickness. Considering a liquid Reynolds number of 3300 as the transition Reynolds number, as determined previously by Karimi and Kawaji (1996), Fig. 2a shows a smooth-laminar film in a developing flow region (Run 1), at 50 cm from the liquid inlet; while Fig. 2b–d depict, respectively, a wavy-laminar film (Run 3), a laminar-to-turbulent transition film (Run 4), and a wavy-turbulent film (Run 6) in a fully developed flow region, at 150 cm from the liquid inlet. Effects of counter-current interfacial shear on film thickness and stream-wise velocity fluctuations are shown in Fig. 3a and b.

From the examination of these figures and other experimental data analyzed, the following observations can be made.

1. The presence of small amplitude ripples on the liquid films does not have a significant effect on the flow structure of liquid or stream-wise velocities, u, close to the solid surface. This is more evident in a developing flow region (Run 1, $L = 50$ cm) even for regions close to the interface. There, only small variations in stream-wise velocity components were obtained under a significant portion of the liquid film as shown in Fig. 2a, because the film was fairly smooth.

   As the liquid film travels further down the tube ($L = 150$ cm), the interfacial waves develop into larger amplitude waves. At this location:
2. Almost all of the local stream-wise velocities exhibited significant resemblance to the film thickness fluctuations. Furthermore, the resemblance grew stronger as the distance from the solid wall, y, increased. The stream-wise velocity does not follow the trends in film thickness exactly, but its magnitude increases with both increases in film thickness and distance from the wall, y, except for large amplitude waves with flat velocity profiles. Under the large amplitude waves, the stream-wise velocities at different distances from the wall approach the

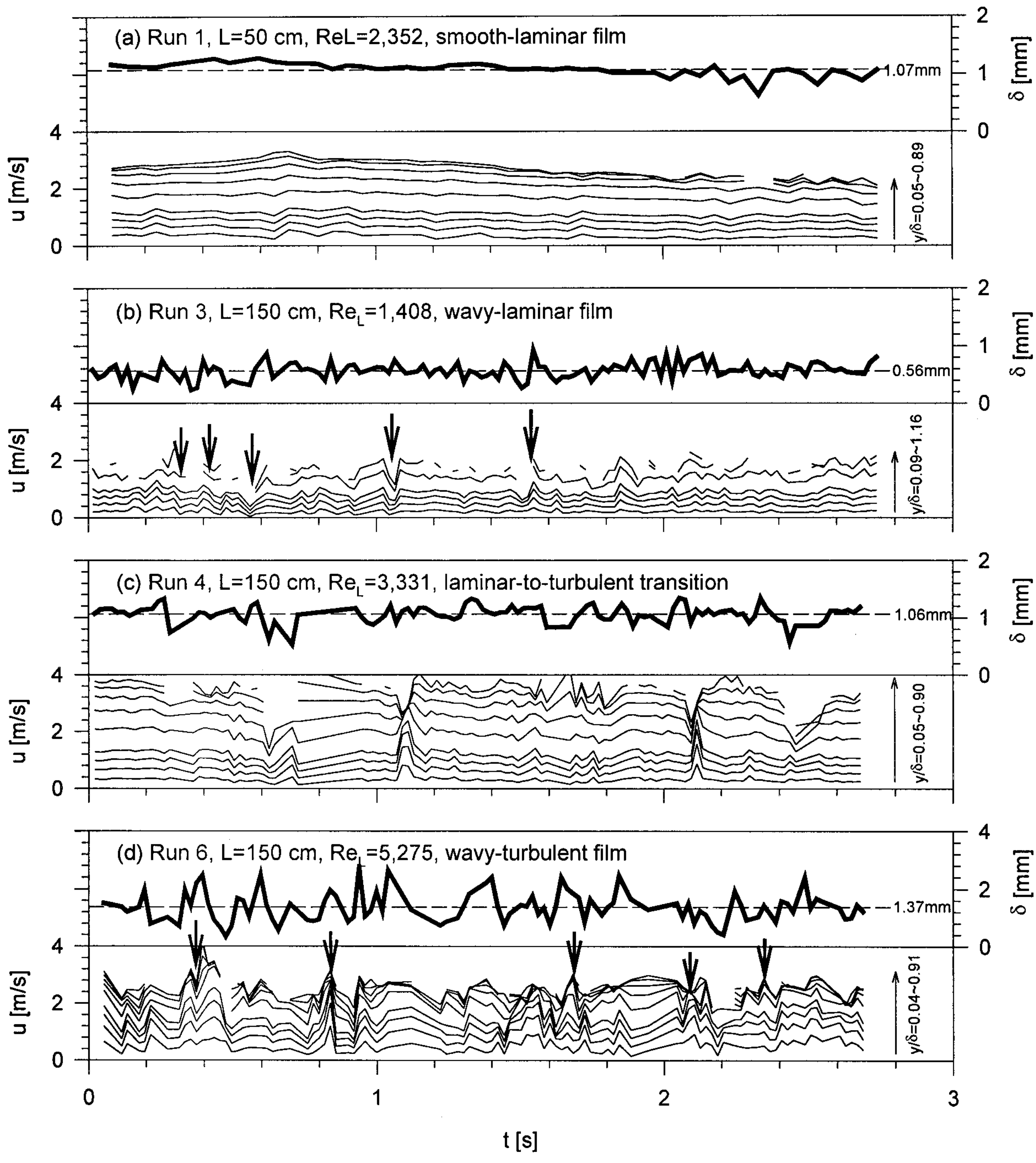

Fig. 2. Simultaneous measurements of liquid film thickness and local stream-wise velocity fluctuations for different flow conditions.

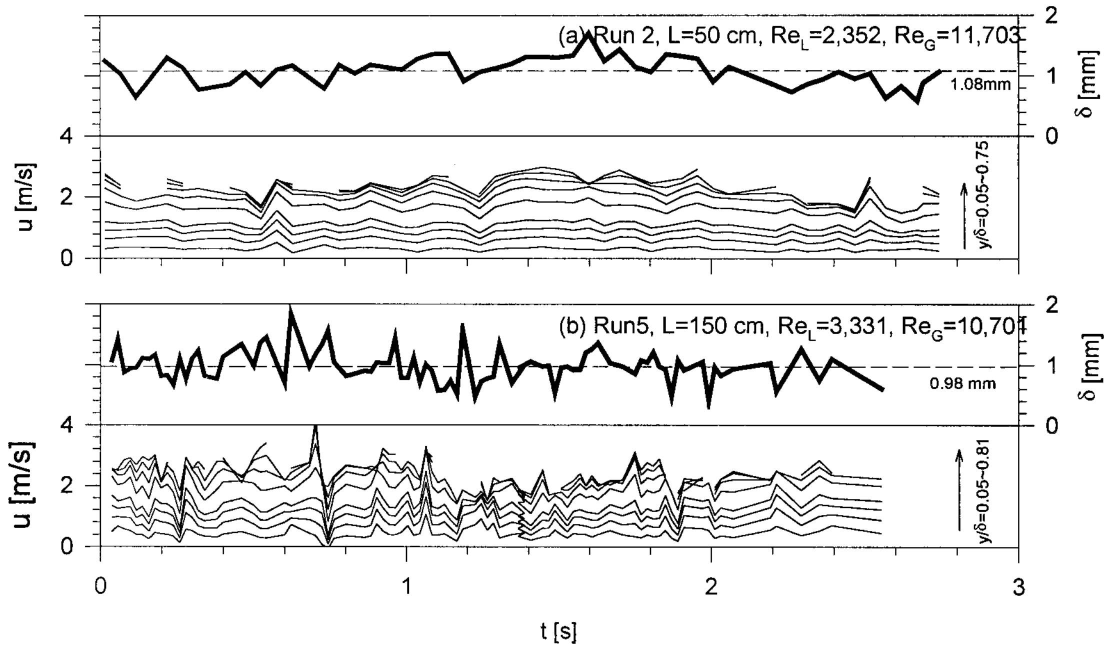

Fig. 3. Simultaneous liquid film thickness and local stream-wise velocity measurements for different flow conditions at the onset of flooding.

same value particularly in regions close to the interface as indicated, for example, in Fig. 2d by arrows.

3. In a wavy-laminar film (e.g., Run 3), the effect of large-amplitude interfacial waves could be sensed even very close to the wall, $y/\bar{\delta} \leq 0.09$. This is shown in Fig. 2b and is probably due to the very small liquid film thickness at this low Reynolds number.
4. At laminar-to-turbulent transition condition (e.g., Run 4), the film could be divided into two distinct regions. The smooth film region where the interface is fairly smooth with insignificant changes in the stream-wise velocity close to the wall, and the wavy region where significant changes in the stream-wise velocity could be observed deep into the liquid film, $y/\bar{\delta} \leq 0.05$, as shown in Fig. 2c.
5. For fully turbulent liquid films (e.g., Run 6), the liquid film is covered completely with a wide spectrum of waves. As shown in Fig. 2d, the interfacial waves induce significant changes in the stream-wise velocity even very close to the wall, $y/\bar{\delta} \leq 0.04$, for almost all parts of the liquid film, regardless of the wave amplitude. There, the stream-wise velocity within the substrate is influenced by the wave-induced turbulence.
6. With the counter-current flow of gas, near the onset of flooding, the waviness of the liquid film markedly increased and this caused greater fluctuations in the stream-wise velocity across the entire film. The effect of counter-current interfacial shear penetrated deeper into the liquid film due to greater fluctuations in the film thickness and significant changes in the stream-wise velocity fluctuations could be observed, particularly at 150 cm from the liquid inlet (run 5 in Fig. 3b), in comparison with the data for run 4 shown in Fig. 2c.

3.2. Turbulence structure of falling liquid films

Local stream-wise velocity fluctuations, u'/U, (where u' is the RMS amplitude of stream-wise velocity fluctuations and U is the time-averaged mean velocity of the liquid film) are calculated and shown in Fig. 4a–d, as a function of the distance from the wall for different liquid and gas Reynolds numbers at locations of 50 and 150 cm from the liquid inlet. As indicated, all of the distributions start with a large gradient at the wall; however, the rate of change in the velocity fluctuation amplitude diminishes beyond $y/\bar{\delta} > 0.2$. Although the counter-current interfacial shear increased the velocity fluctuations at both locations (Fig. 4a and c), the effect was greater at the 150 cm location and extended very close to the tube wall as shown in Fig. 4c. This is due to the presence of larger amplitude waves at the liquid surface at this location.

Now that the velocity fluctuations within falling liquid films have been compared under different film flow conditions, it would be interesting to compare transition to turbulent flow in a liquid film with that of single-phase pipe flow. Table 2 compares the measured average liquid film velocities, U_{FF}, with the average velocity, $U_{SP} = 0.139$ m/s, for single-phase flow in a 50.8 mm ID pipe, corresponding to the laminar-to-turbulent transition Reynolds number of 4000.

With average velocities an order of magnitude larger than that of the corresponding single-

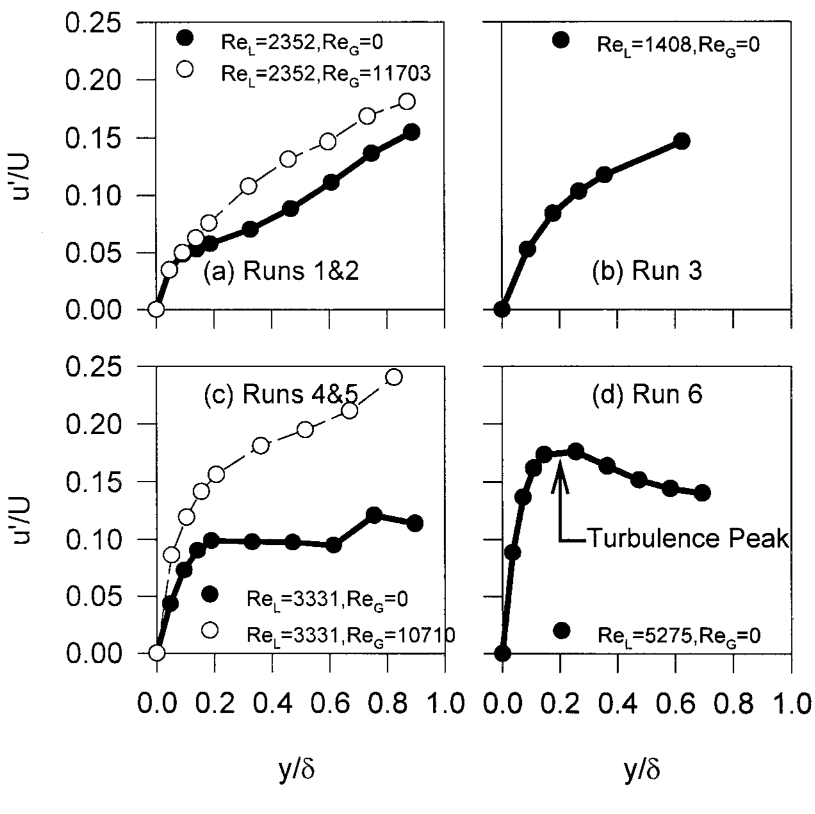

Fig. 4. Variation of velocity fluctuation amplitude with distance from the wall for different liquid and gas Reynolds numbers.

Table 2
Comparison of average velocities

Re	U_{FF} (m/s)	U_{FF}/U_{SP}
1408	1.16	8.34
3331	2.39	17.19
5275	2.36	16.98

phase flow as listed in Table 2, and with the surface waves continuously providing vigorous disturbances as shown in Figs. 2 and 3, falling films are expected more likely to become turbulent at a much lower Reynolds number than 4,000 in pipe flow. However, the present results suggest otherwise.

In single-phase pipe flow, turbulence is generated near the wall in the form of bursts which generate large eddies. The turbulence energy is transferred from the larger eddies to smaller eddies and eventually dissipated by a viscous mechanism. On the other hand, the eddy size in falling liquid films is restricted by the liquid film thickness, which is very small. Furthermore, the free surface has two competing effects on turbulence depending on the waviness of the film surface. The smooth free surface tends to damp out any abrupt disturbances coming from near the wall, which may be regarded as *wall turbulence*. However, the wavy free surface induces fluctuations in film thickness and both surface-normal and stream-wise liquid velocities, which may be regarded as *wave-induced turbulence*. The significance of each mechanism depends on the wave amplitude as well as on other factors, such as liquid and gas Reynolds numbers, liquid properties and physical geometry.

Hence, with these inherent characteristics of falling liquid films, turbulence is difficult to be initiated and sustained in smooth films at small Reynolds numbers. However, once the film becomes wavy and turbulent, the turbulence intensity distributions are amplified and generally greater than those of single-phase pipe flow.

As depicted in Fig. 4b, the amplitude of velocity fluctuations for the wavy-laminar film (Run 3) increases continuously towards the liquid surface. For such a low Reynolds number film, the stream-wise velocity fluctuations arise only due to the fluctuations in the film thickness. They are certainly not wall-generated turbulence because the Reynolds number is too low, but the velocity fluctuations would be expected to have a non-negligible effect on interfacial or wall-liquid heat and mass transfer rates.

On the other hand, the wavy-turbulent film in the developed flow region (Run 6, Fig. 4d) shows a behavior similar to that of pipe flow. The turbulence intensity distribution shows a single peak near the tube wall. At this Reynolds number, the peak is similar to that of turbulent pipe flow and is partly due to a high degree of turbulence originating near the wall and partly due to the large fluctuations in the film thickness caused by the passage of interfacial waves. The similarity to a pipe flow suggests that there may be turbulent bursts (ejections and sweep) occurring near the tube wall, which may cause vortex motion within the liquid film.

Fig. 5a and b show sequences of images obtained at 744 frames per second for typical large amplitude waves in a liquid film falling freely without any adjacent gas flow at a Reynolds

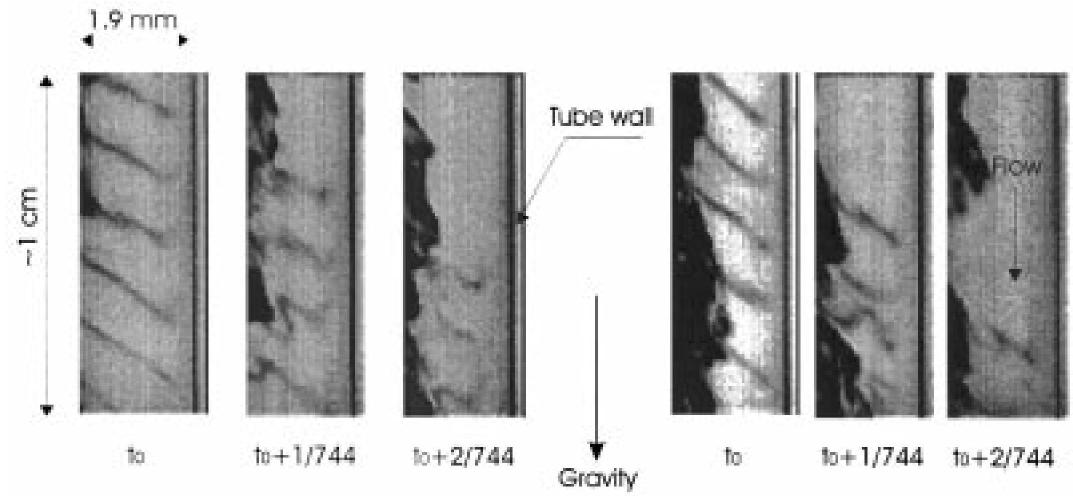

Fig. 5. Sequences of images obtained for typical large amplitude waves in a freely falling film ($Re_L = 5275$, $L = 150$ cm).

number of 5275. Multiple-dye traces were created in the film using an Excimer laser and a lens array, in order to explore the internal flow structure of large amplitude waves more precisely. As can be seen from the images, dye traces are linearly formed in the wave. Linear appearance of the dye traces with almost identical slopes is due to the scanning process of the digital video camera used in this work, and indicates that a flat velocity profile prevails within a major part of the wave. This phenomenon has been recently described in detail in Karimi and Kawaji (1998). However, some patches of liquid appear to be clearly ejected from the tube wall and move toward the gas–liquid interface as time elapses. These ejections twist the trace profile under the large wave and induce rolling eddies to form, which could renew both the wall and interface regions of the liquid film. Qualitative analyses of the images obtained in this work indicate that these types of ejections penetrate further across the liquid film at higher liquid Reynolds numbers when counter-current interfacial shear is applied. Although similar observations of surface renewal motions in a wavy-stratified flow in a horizontal channel have been reported by Rashidi and Banerjee (1990), Komori et al. (1993), and by Lorencez et al. (1997a, 1997b), to the authors' knowledge, this is the first time such vortex motions have been directly captured in a falling liquid film.

Images in Fig. 5 only display a very small portion, about 10 mm in length, of a large wave unit, typically over 100 mm in length. Since the eddy size would be of the order of film thickness, which is much smaller in scale than the wavelength, it is reasonable to think that more than several vortices of varying sizes simultaneously exist under a single large wave as illustrated in Fig. 6.

A few large eddy cells were also detected at laminar flow conditions. The evolution of a typical large eddy cell within a large amplitude wave is shown in Fig. 7 for a liquid Reynolds number of 1824 at the onset of flooding. As shown in this figure, the large wave approaches the measuring point with a significant reduction in the film thickness followed by a sudden increase in the film thickness. As seen from the sequence of images, a large eddy formed in the

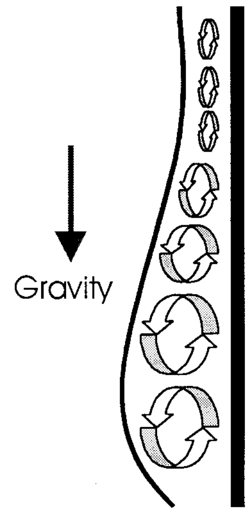

Fig. 6. Diagram of a large wave associated with a number of circulation eddies.

wave front that grew larger in size to almost match the wavy film thickness. The axis of rotating eddy is parallel to the tube wall and normal to the direction of liquid flow. The existence of a vortex under a large amplitude wave in a falling laminar film at low liquid Reynolds number has been numerically predicted by Moalem Maron et al. (1989), Yu et al. (1995), Matsumoto and Koyanagi (1996). Jayanti and Hewitt (1997) also predicted the

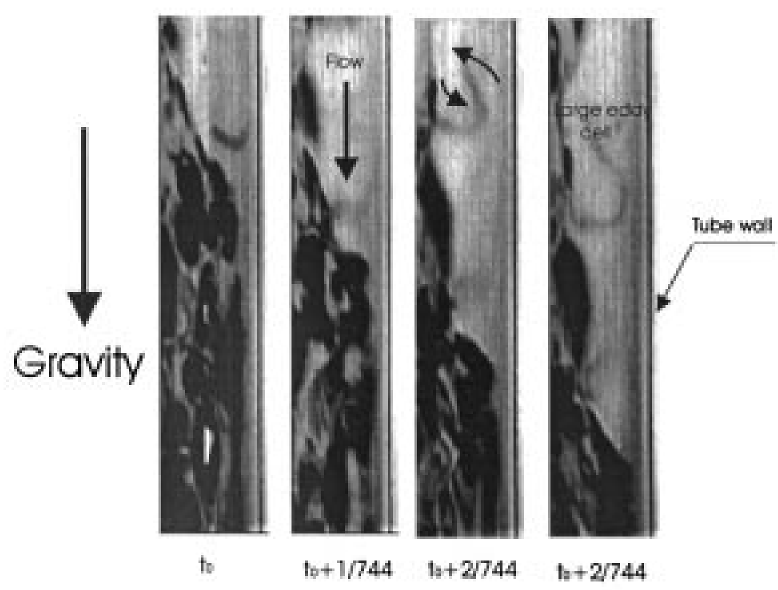

Fig. 7. Evolution of a typical large eddy cell within a large amplitude wave at 150 cm from the liquid inlet and at the onset of flooding ($Re_L = 1824$).

evolution of vortices under disturbance waves through numerical simulation of a prescribed wavy film subjected to interfacial shear under both laminar and turbulent conditions. In the present work, the vortex formation may have been further influenced by the effect of counter-current interfacial shear acting on the interface at the onset of flooding.

The detailed information on the frequency of appearance of these ejections or surface renewal eddies, their time and length scales, the ejection characteristics, penetration depth and direction, and the interfacial shear stress effects has yet to be obtained for both laminar and turbulent wavy films.

3.3. Mass transfer in falling films

The notion of existence of several surface renewal motions under a large wave can be further examined through available experimental mass transfer coefficients. Considering a random distribution of eddy ages at the liquid interface, Danckwerts (1951) proposed his surface renewal theory as

$$K_L = \sqrt{DS} \tag{1}$$

where K_L is the liquid side mass transfer coefficient, D is diffusivity and S is the surface renewal frequency.

If every large wave can hold on average N large vortices, the surface renewal frequency for a falling liquid film would be $S = Nf_w$ where f_w is the frequency of large waves. Obviously, the value of N would depend on the wave characteristics. Different values of N can be tested in Eq. (1), by comparing the resulting liquid side mass transfer coefficients with various empirical correlations, which have been previously developed based on a variety of gas absorption data obtained for falling films, as shown in Fig. 8. These correlations are indicated by solid and broken lines, while the predictions based on Eq. (1) and the frequencies of large-amplitude waves measured at two different liquid Reynolds numbers in the present experiments (4 and 14 Hz for runs 3 and 6, respectively) are shown by symbols. As evident in this figure, the best values of N, which give relatively good agreement in laminar flow ($Re_L = 1408$) and turbulent flow ($Re_L = 5275$) are about 4 and 9, respectively. This suggests that a large amplitude wave is potentially able to generate many surface-renewing vortices over its wavelength. Although the value of N for wavy-laminar film is much smaller than that for a turbulent film, it is still considerably higher than 1, suggesting the presence of more than one vortex under a large-amplitude wave.

It is worth mentioning that most of the data on mass transfer coefficients in wavy films (including those in Fig. 8) are reported in terms of an average value over the entire test section including the smooth entry region, the developing wave region and the fully developed wavy flow region. Thus, the actual values of vortices existing under fully developed waves may be greater than the values of N estimated above.

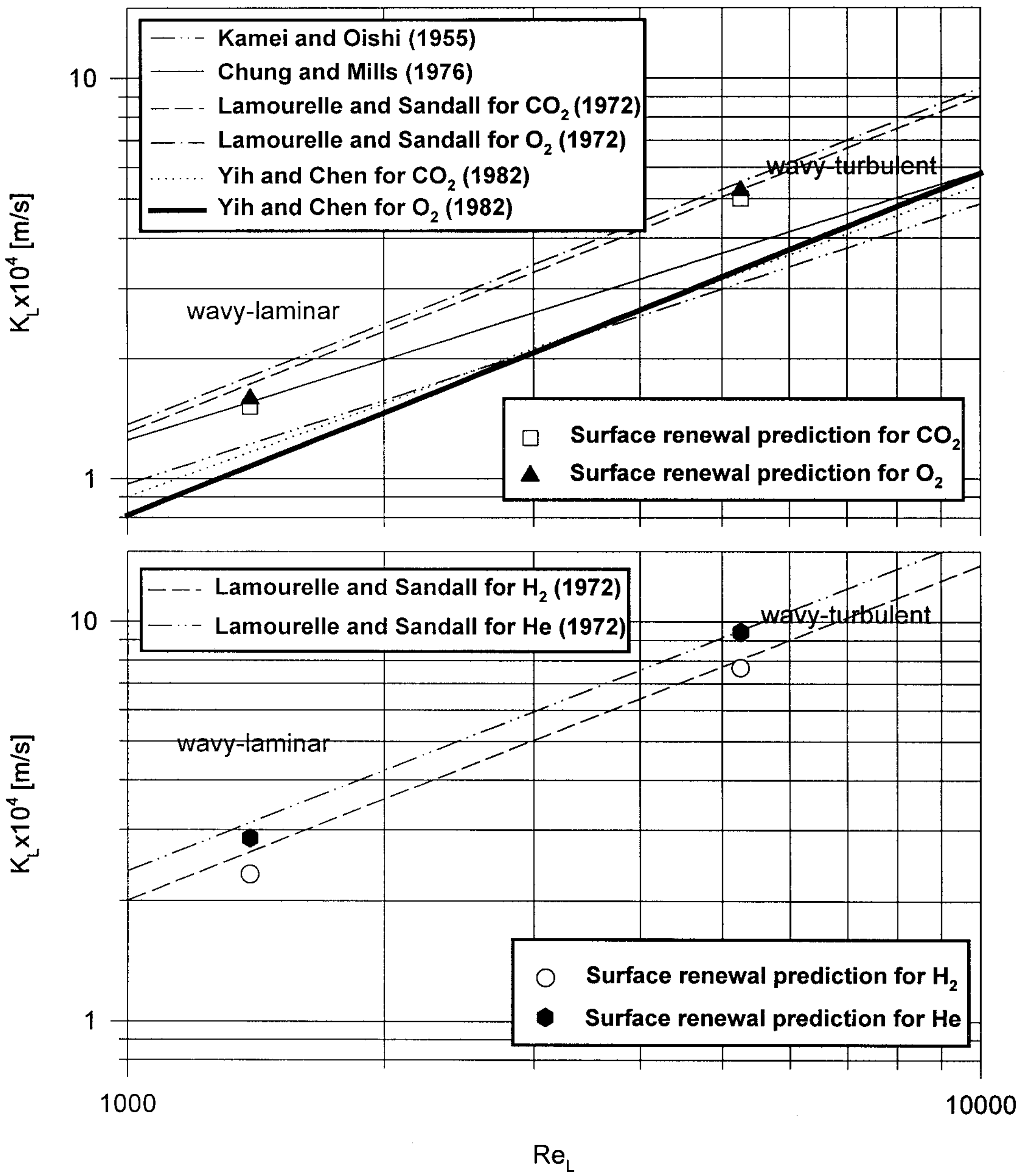

Fig. 8. Comparison of empirical correlations for mass transfer coefficients with Danckwerts surface renewal model.

4. Conclusions

Local stream-wise velocity variations and film thickness fluctuations were simultaneously measured, and turbulence structures were investigated for falling liquid films over a wide range of liquid and gas Reynolds numbers. An insignificant role of ripples on the near wall hydrodynamics was found in a developing wave region at $L = 50$ cm from the liquid inlet. In the developed wavy film region ($L = 150$ cm), however, the wave effect could easily be sensed close to the solid wall in both wavy-laminar and turbulent films and is only important in the wavy part of the film in transition conditions. Flow visualization experiments revealed the occurrence of circulatory motions with significant velocities normal to the tube wall under large waves, which may be the dominant mechanism for wall-to-liquid and interfacial transport phenomena for wavy films. The available mass transfer coefficient data obtained in various gas absorption experiments appear to suggest the existence of about 4 to 9 vortices under a large amplitude wave in wavy laminar and turbulent falling films.

Acknowledgements

The authors would like to acknowledge financial support for this work provided by the Natural Sciences and Engineering Research Council of Canada and Japan Atomic Energy Research Institute, as well as a graduate fellowship (for G. Karimi) from the Shiraz University, Iran.

References

Banerjee, S., Rhodes, E., Scott, D.S., 1967. Mass transfer to falling wavy liquid films at low Reynolds numbers. Chem. Eng. Sci. 22, 43–47.

Chung, D.K., Mills, A.F., 1976. Experimental study of gas absorption into turbulent falling films of water and ethylene glycol-water mixtures. Int. J. Heat Mass Transfer 19, 51–59.

Danckwerts, P.V., 1951. Significance of liquid-film coefficients in gas absorption. Ind. Eng. Chem. 43, 1460–1467.

Emmert, R.E., Pigford, R.L., 1954. A study of gas absorption in falling liquid films. Chem. Eng. Prog. 50, 87–93.

Fortescue, G.E., Pearson, J.R., 1967. On gas absorption into a turbulent liquid. Chem. Eng. Sci. 22, 1163–1176.

Henstock, W.H., Hanratty, T.J., 1979. Gas absorption by a liquid layer flowing on the wall of a pipe. AIChE J. 25, 122–131.

Higbie, R., 1935. The rate of absorption of a pure gas into a still liquid during short period of exposure. Trans. AIChE J. 31, 365–388.

Jayanti, S., Hewitt, G.F., 1997. Hydrodynamics and heat transfer in wavy annular gas–liquid flow: a computational fluid dynamic study. Int. J. Heat Mass Transfer 10, 2445–2460.

Kamei, S., Oishi, J., 1955. Mass and heat transfer in a falling liquid film of wetted wall tower. Mem. Fac. Eng. (Kyoto Univ.) 17, 277.

Karimi, G., Kawaji, M., 1996. A study of hydrodynamic characteristics of non-conductive falling films in counter-current annular flow. In: Thirty-first National Heat Transfer Conference, Aug. 3–6, 1996, Houston, Texas, HTD-326, 205–221.

Karimi, G., Kawaji, M., 1997. Flooding in vertical counter-current annular flow. In: Proceeding of the Eighth International Topical Meeting on Nuclear Reactor Thermal-hydraulics NURETH-8, Kyoto, Japan, Sept. 30–Oct. 4, 1997. vol. 4, 1637–1646.

Karimi, G., Kawaji, M., 1998. An experimental study of free falling films in a vertical tube. Chem. Eng. Sci. 53, 3501–3512.

Komori, S., Nagaosa, R., Murakami, Y., 1998. Turbulence structure and mass transfer across a sheared air–water interface in wind-driven turbulence. J. Fluid Mech. 249, 161–183.

Lamurelle, A.P., Sandall, O.C., 1972. Gas absorption into a turbulent liquid. Chem. Eng. Sci. 19, 1035–1042.

Lorencez, C., Nasr-Esfahany, M., Kawaji, M., Ohja, M., 1997a. Liquid turbulence structure at a sheared and wavy gas–liquid interface. Int. J. Multiphase Flow 23 (2), 205–226.

Lorencez, C., Nasr-Esfahany, M., Kawaji, M., 1997b. Turbulence structure and prediction of interfacial heat and mass transfer in wavy-stratified flow. AIChE J. 43 (6), 1426–1435.

Moalem Maron, D., Brauner, N., Hewitt, G.F., 1989. Flow patterns in wavy thin films: numerical simulation. Int. Comm. Heat Mass Transfer 16, 655–666.

Matsumoto, Y., Koyanagi, T., 1996. Unsteady flow structure of liquid film falling down walls. In: Proceeding of the Japan–US Seminar on Two-Phase Flow Dynamics, July 15–20, 1996, Fukuoka, Japan, 121–127.

Rashidi, M., Banerjee, S., 1990. Streak characteristics and behavior near wall and interface in open channel flows. Trans. of the ASME 112, 164–170.

Seban, R., Faghri, A., 1978. Wave effects on the transport of falling laminar liquid films. Trans. ASME J. Heat Transfer 100, 1.

Wasden, F.K., Dukler, A.E., 1992. An experimental study of mass transfer from a wall into a wavy falling film. Chem. Eng. Sci. 47, 323–331.

Yih, S.M., Chen, C.H., 1982. Heat transfer in the thermal entrance region of a turbulent falling liquid film undergoing heat or evaporation. Proc. Seventh Int. Heat Transfer Conf. 3, 125–130.

Yoshimura, P.N., Nosoko, T., Nagata, T., 1996. Enhancement of mass transfer into a falling laminar liquid film by two-dimensional surface waves-some experimental observations and modelling. Chem. Eng. Sci. 51 (8), 1231–1240.

Yu, L., Wasden, F., Dukler, A.E., Balakotaian, V., 1995. Non-linear evolution of waves on falling films at high Reynolds numbers. Physics of Fluids 7 (8), 1886–1902.